International Journal of Remote Sensing
Vol. 31, Nos. 7–8, April 2010, 2151–2157

Taylor & Francis
Taylor & Francis Group

Soil surface illumination at micro-relief scale and soil BRDF data collected by a hyperspectral camera

JERZY CIERNIEWSKI*†, ARNON KARNIELI‡, ITTAI HERRMANN‡, SŁAWOMIR KRÓLEWICZ† and KRZYSZTOF KUŚNIEREK†

†Department of Soil Science and Remote Sensing of Soils, Adam Mickiewicz University in Poznań, Dzięgielowa 27, Poznań 61-680 Poland

‡Remote Sensing Laboratory, Jacob Blaustein Institutes for Desert Research, Ben Gurion University of the Negev, Sede Boker Campus 84990, Israel

(*Received 10 July 2009; in final form 11 January 2010*)

The results of the paper draw attention to the fact that the hyperspectral image of soil surface at micro-relief scale may display variation in the soil spectral shape due to illumination conditions of the surface. The image of an extremely rough cultivated soil surface, very deeply ploughed, was obtained by a hyperspectral camera, in the range of 0.4–1.0 μm with 0.67–0.74 nm spectral resolution. It was found that the soil reflectance spectra of the studied surface, illuminated by the direct sunbeams, are clearly convex with distinct absorption features. Furthermore, the soil normalized reflectance spectra were used to distinguish the subtlety of the analysed shaded soil spectra shape. They show that depressions caused by the absorption features of O_2 and H_2O, contained in the atmosphere above directly illuminated soil fragments, transform into peaks, if the same soil is deeply shaded.

1. Introduction

Spectral reflectance in the visible and near-infrared region is used to detect different Earth objects, to separate them, and to infer their chemical, physical, or biological properties. The reflectance spectrum of bare soils, like many natural and the man-made objects, depends on absorption of incident radiation in discrete wavelength ranges caused by substances included in a soil material. These soil components are mainly clay and iron oxide minerals, organic matter, and various forms of water (hydration, hygroscopic, and free) (Ben-Dor *et al*. 1998). The absorption features of the substances significantly affect the shape of a soil reflectance spectrum. Numerous examples of the soil hyperspectral reflectance experiments show that physical features of soils, such as irregularities of their surfaces, caused by the soil texture, aggregates and microrelief configuration, as well as by their illumination and observation conditions, influence their spectra (Cierniewski *et al*. 2004, Chappell *et al*. 2006).

The goal of the paper is to draw attention to the fact that selected parts of the soil hyperspectral image at micro-relief scale may display variation in the spectra shape due to illumination conditions of the soil surface. The paper focuses on the visible and near-infrared range, where absorption features of chemical and physical chromophores occur in a lower intensity than for longer wavelengths of the optical range, and

*Corresponding author. Email: ciernje@amu.edu.pl

International Journal of Remote Sensing
ISSN 0143-1161 print/ISSN 1366-5901 online
http://www.tandf.co.uk/journals
DOI: 10.1080/01431161003610281

where their influence is less frequently identified. This objective was implemented in conjunction with a high spatial resolution hyperspectral camera.

2. Methods

The experiment was conducted on a cultivated field near Sede Boker in Israel (30°51′26′N, 34°47′09′E). This area is characterized by loessial substrate (Issar *et al*. 1984) and the test plot was located on an extremely rough, deeply ploughed, cultivated soil surface.

The hyperspectral bidirectional reflectance features of the surface and a Spectralon® white reference panel were recorded using Spectral Camera HS manufactured by Specim in a spectral range of 0.4–1.0 μm with 0.67–0.74 nm spectral resolution. The camera, equipped with a pushbroom line scanner, observes a target in the across and along scan directions with a 28° and 90° field-of-view, respectively. The instrument was fixed on a 4-m height construction that enables to obtain the hyperspectral image of a 8×2 m plot (figure 1). The image was recorded on 25 August 2008 at the high solar

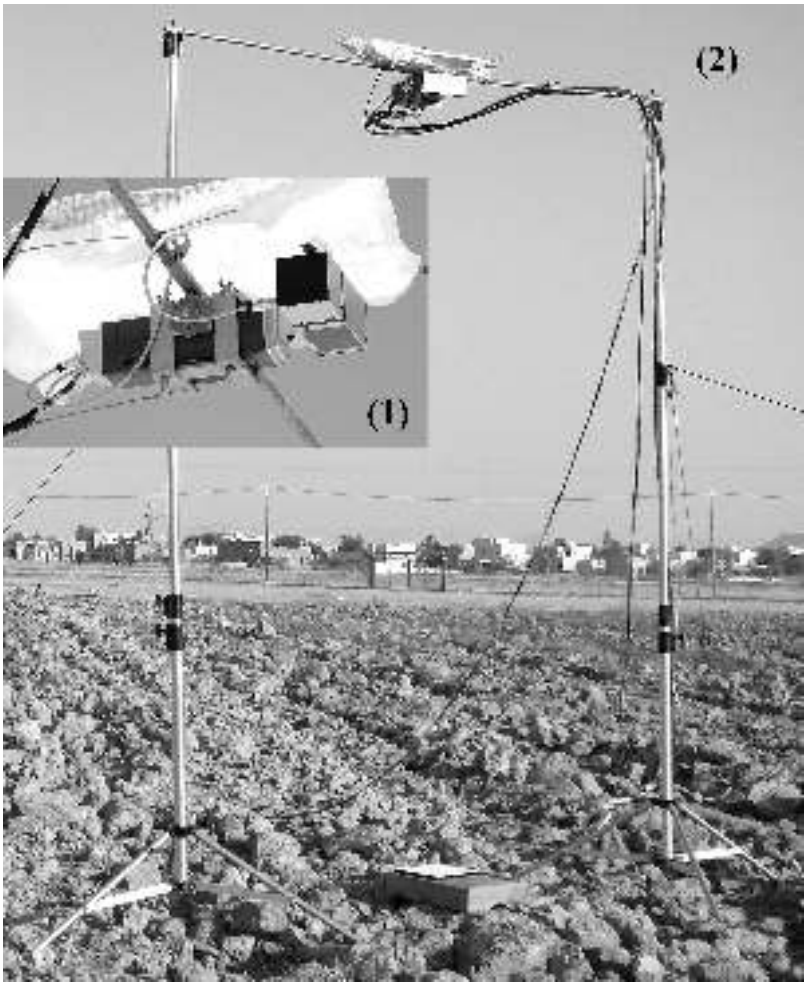

Figure 1. (1) The spectral camera HS; (2) set-up of the camera on a 4 m height construction.

Figure 2. Setup of the 3D Konica–Minolta VIVID910 laser scanner.

zenith angle of 75°, providing a high variation of the surface illumination. To reduce the impact of the view direction on the surface reflectance, only the central part of the image, of 0.91×0.99 m, was selected.

Surface roughness measurements were carried out with a Konica–Minolta VIVID-910 laser scanner. The scanner was placed on a tripod that was moved around to read a 1 m^2 plot from four different directions. Due to the scanner's working conditions, the 3D measurements were conducted at night using a fluorescent lamp (figure 2). The 3D scanner source data were transformed to a set of points with X, Y and Z coordinates. A digital elevation model (DEM) of the obtained surface was computed with 1 mm horizontal and vertical spatial resolutions.

The central part of the hyperspectral image was georeferenced and orthorectified using the DEM. The raw radiance data were transformed to reflectance values utilizing Spectralon reference panel data by the flat-field correction method.

Twelve sampled points, 5×5 pixels size each, were chosen in the hyperspectral sub-image. Their size was large enough to describe accurately a slope inclination and aspect of soil clods and aggregate. Four of these points incorporated with sunlit soil fragments (L) and eight with shaded ones (S) were tested. Based on the DEM and the values of solar and view zenith and horizontal angles noted in the process of the hyperspectral measurements, the direct sunbeams incidence angle γ_i and the view angle γ_v, of the tested surface at given point, both with respect to the normal of the point, were calculated only for the sunlit soil fragments. In addition, the solid angle ϕ_{di} values describing a part of the sky hemisphere, which was the only source of illumination of shaded soil fragments, were computed.

The textural composition of the soil surface material was analysed in the laboratory using a hydrometer, the organic carbon content by Walkley Black's method,

calcium carbonate equivalent by Piper's method, and total 'free' iron oxide by the Citrate–Dithionite–Bicarbonate (CDB) method of Mehra and Jackson (Sparks *et al.* 1996).

3. Results and discussion

Soil properties that significantly influence the reflectance features are summarized in table 1.

The DEM was used to quantitatively characterize the shape of the studied surface using the following indices: the height standard deviation, the ratio of the total surface area to the total projected area, and the height variogram sill and range parameters. Their values are: 59 mm, 1.76, 115 mm, and 1738 mm, respectively.

For each measurement point, an individual reflectance curve was extracted from the reflectance hyperspectral cube in places marked in figure 3. The reflectance of each of the analysed soil fragments was calculated as the ratio of the radiation reflected from a given soil fragment to the radiation reflected from the Spectralon panel positioned horizontally and illuminated at the constant solar zenith angle of 75°. The reflectance data were limited to 900 nm due to spectral noise in the longer wavelengths. The angles describing condition of the soil surface fragments illumination are presented in table 2.

The curves, presented in figure 4(*a*), show that the curves of the higher illuminated points, described by the γ_i, are more convex and are characterized by the higher reflectance level. The spectra for the shaded soil fragments are less convex. They lose their convex features if they are characterized by ϕ_{di} lower than about 4.5 sr (S5–S8). The spectra that characterize the image points illuminated directly by the sunbeams (L1–L4) as well as the points located within a light shadow (S1–S3, described by the ϕ_{di} higher than about 5.5 sr), show absorption features at around of 0.76 μm and 0.82 μm. The absorption at shorter wavelengths and longer ones is caused by air components over the analysed surface, O_2 and H_2O, respectively (Ben-Dor *et al.* 1998, Hatchell 1999). The spectra, relating to the points situated already inside a dark shadow (S4–S8) do not show these features.

The reflectance spectra, discussed above, were then transformed into their normalized form, calculated by a max–min function (Selige *et al.* 2006), to distinguish their spectral shape subtlety. The normalized spectra show that the absorption features, expressed by depressions in the curves related to places of high illumination (L1–L4, S1–S3) are replaced by their peaks for curves characterizing places of dark shadow (S6–S8) (figure 4(*b*)). Furthermore, the latter spectra are evidently more concave in the region over 0.8 μm. Following Georgieva *et al.* (2004) who claim that the oxygen

Table 1. Properties of the soil surface.

Content of:	Value
Sand (2–0.05 mm)	48%
Silt (0.05–0.002 mm)	40%
Clay (< 0.002 mm)	12%
Organic carbon	0.92%
$CaCO_3$	28.1%
Fe_2O_3	1.52%
Soil Munsell dry colour	10YR7/4

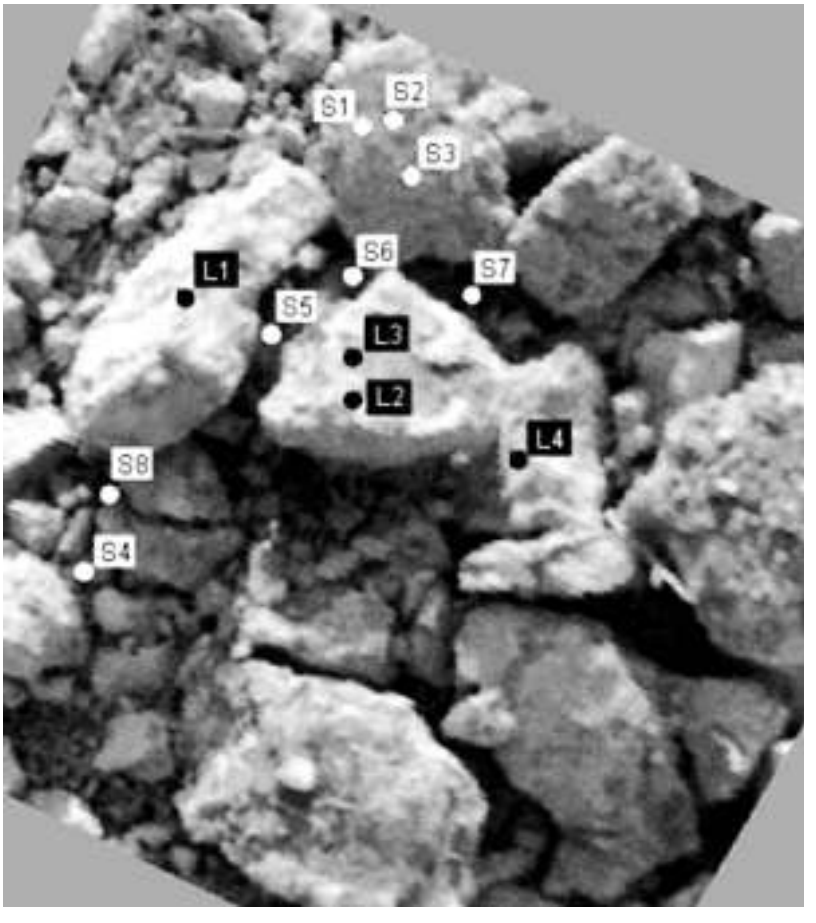

Figure 3. A set of 12 measurement points selected in the hyperspectral sub-image.

Table 2. Illumination and view angles characterizing the measurement places, sunlit (L) and shaded (S).

Symbol	Direct sunbeams incidence angle (°)	View angle (°)	Solid angle (sr)
L1	43.0	71.2	–
L2	54.9	43.6	–
L3	63.4	26.8	–
L4	65.4	41.7	–
S1	–	35.4	5.75
S2	–	15.0	5.69
S3	–	27.2	5.40
S4	–	11.7	4.94
S5	–	72.8	4.51
S6	–	47.6	4.36
S7	–	42.7	4.26
S8	–	81.8	3.99

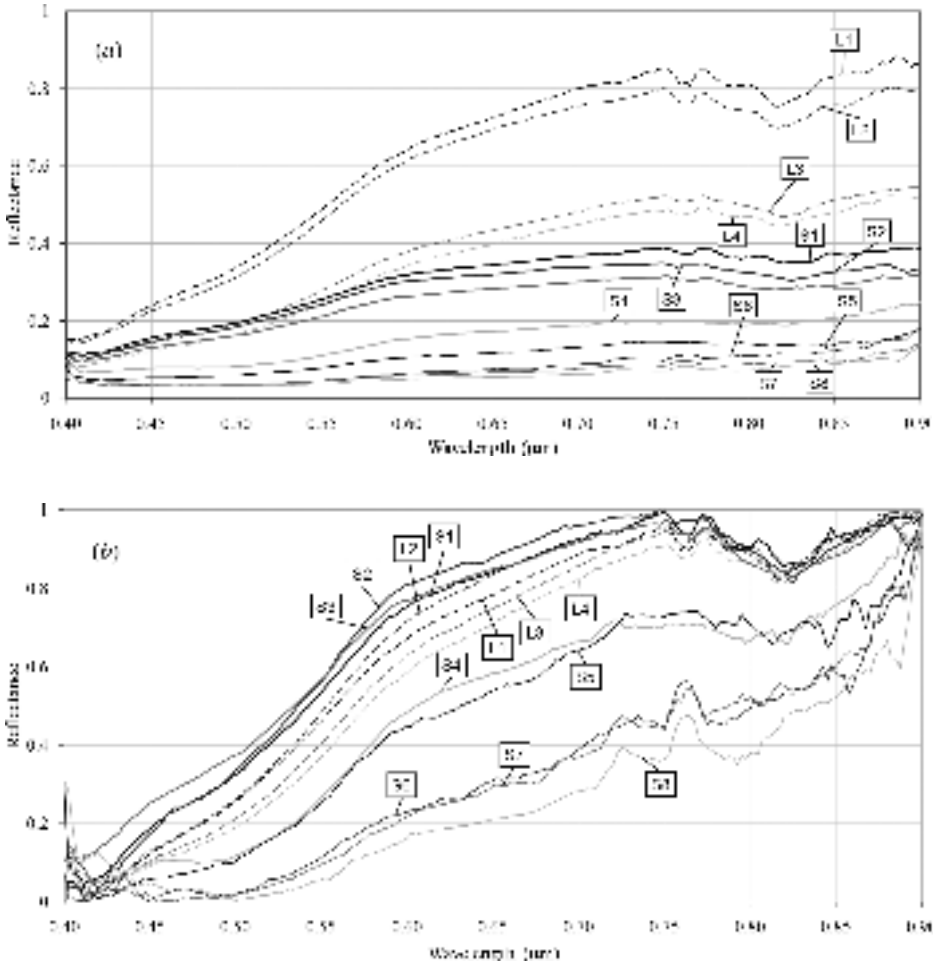

Figure 4. (*a*) The reflectance spectra of the measured points (sunlit [L] and shaded [S]). (*b*) The same spectral curves normalized by the min–max method.

absorption band in the spectral region of 765.5–770 nm is sensitive to temperature changes, it is hypothesized that the variation in reflectance in this band may be addressed by temperature variation of the atmosphere over the analysed surface. It is further assumed that the lower content of H_2O inside the atmosphere column over the shaded soil fragments, of a lower temperature, is the reason for the lower absorption features at around 0.82 μm of the shaded soil fragments.

4. Conclusions

The results presented in this paper, carried out on a limited set of soil hyperspectral data at micro-relief scale, reveal that variation in soil surface illumination conditions not only affects the level of the soil spectra, but also their shape. The studied soil reflectance spectra of soil fragments illuminated by the direct sunbeams are convex in the range of 0.4–0.9 μm with distinct absorption features. Using the normalized

reflectance to distinguish the shape subtlety of the analysed soil spectra, it was found that depressions caused by the absorption features of O_2 and H_2O contained in the atmosphere column between the studied surface and the sensor, change into peaks if the same soil is observed by the hyperspectral sensor within dark shadow.

Acknowledgements

This work was supported by the 'Sixth EU Framework Programme – Transnational Access implemented as Specific Support Action – Dryland Research' (EC contract number: 026064). The authors wish to thank Aleksander Goldberg for his help in the field measurements.

References

Ben-Dor, E., Irons, J.R. and Epema, G.F., 1998, Soil reflectance. In *Remote Sensing for the Earth Sciences*, A.N. Rencz (Ed.), pp. 111–186 (New York: John Wiley & Sons).

Cierniewski, J., Gdala, T. and Karnieli, A., 2004, A hemispherical–directional reflectance model as a tool for understanding image distinctions between cultivated and uncultivated bare surfaces. *Remote Sensing of Environment*, **90**, pp. 505–523.

Georgieva, E., Wilson, E., Miodek, M. and Heaps, W.S., 2004, Experimental data on O_2 absorption using Fabry–Perot-based optical setup for remote sensing atmospheric observations. *Proceedings of SPIE*, **5542**, pp. 195–206.

Chappell, A., Zobeck, T.M. and Brunner, G., 2006, Using bi-directional soil spectral reflectance to model soil surface changes induced by rainfall and wind-tunnel abrasion. *Remote Sensing of Environment*, **102**, pp. 328–343.

Hatchell, D.C. (Ed.), 1999, *ASD Technical Guide*, 4th ed. (Boulder, CO: Analytical Spectral Devices Inc.).

Issar, A., Karnieli, A., Bruins, H.J. and Gilead, I., 1984, The quanternary geology of Sede-Zin, Negev, Israel. *Israel Journal of Earth Science*, **33**, pp. 34–42.

Selige, T., Böhner, J. and Schmidhalter, U., 2006, High resolution topsoil mapping using hyperspectral image and field data in multivariate regression modeling procedures. *Geoderma*, **136**, pp. 235–244.

Sparks, D.L., Page, A.L., Helmke, P.A., Loeppert, R.H., Soltanpour, P.N., Tabatabai, M.A., Johnston, C.T. and Summer, M.E. (Ed.), 1996, *Methods of Soil Analysis. Part 3. Chemical Methods* (Madison, WI: Soil Science Society of America and American Society of Agronomy).